WWJMRD 2023; 9(03): 1-15
www.wwjmrd.com
International Journal
Peer Reviewed Journal
Refereed Journal
Indexed Journal
Impact Factor SJIF 2017: 5.182 2018: 5.51, (ISI) 2020-2021: 1.361
E-ISSN: 2454-6615

Fikereselise Akalu
Department of Civil Engineering, College of Engineering, Assosa University, Assosa, Ethiopia.

Correspondence:
Fikereselise Akalu
Department of Civil Engineering, College of Engineering, Assosa University, Assosa, Ethiopia.

Effect of Land use Land Cover Change on River Flow and Sediment Yield: A Case Study of ABAY Watershed, DABUS Sub-Basin, Ethiopia

Fikereselise Akalu

Abstract
Dabus watershed is facing high erosion rates due to intense rainfall storms, aggravated by the land use land cover change. A significant land use change has been observed in the Dabus watershed. The main objective of this study was to estimate the potential impacts of the land use land cover (LULC) dynamics on hydrological response (stream flow and sediment yield). The land use land spread change examinations were performed using ERDAS Imagine 2015 that was used for further assessment of SWAT. The recreation and affectability examination for each land use was finished by separating the catchment in to 49 sub-watershed and allocating HRUs dependent on different HRU definition. After an affectability investigation, adjustment and approval of SWAT model, the effect of LULC elements on hydrological reaction were assessed with three situations (1986 LULC, 2019 LULC and 2029 LULC). In the Dabus watershed, land spread change beneficially affected displayed watershed reaction because of the change from timberland land to agribusiness land and bush land to developed zone. Reproduction results for the Dabus watershed indicates that becoming developed and developed territories caused in expanded yearly and regular stream and dregs yield in volumes. The mean annual stream flow was increased by 9.02% (129.20–137.74 m^3/s) and the impact on sediment yield amounts to an increase of 25.39% (23.54–45.18 t/ha/yr) due to LULC dynamic forces. The hydrological response was more sensitive to LULC dynamics for the months of Jun to September than others in the year. These outcomes exhibit the convenience of incorporating remote detecting and appropriated hydrologic models using GIS for evaluating watershed conditions and the overall effects of land spread changes on hydrologic reaction in a ceaseless way.

Keywords: LULC, SWAT, ERDAS Imagine 2015, Dabus watershed

1. Introduction
Land use and land cover change (LULC) is unique of the most hazardous environmental problems affecting the quality of soil, land, and water resources upon which humans depend for their sustenance (Chiwa, 2012) . LULC change is one of the most severe impacts that has caused global ecological environmental crises. Around 40-75% of the world's rural land's efficiency is reduced because of land degradation (Joseck et al., 2016). This has a solid effect on the employment of rural societies.

High population and horticultural practices in Ethiopia are commonly witnessed where the country's climate and environmental conditions are conducive. Deforestation, wetland degradation and prairie encroachment have greatly contributed to the change of the land cover. Large scale environmental wonders, for example, exploitation and desertification to provide a settlement space and biodiversity imbalance are outcomes of land utility changes (Sewnet, 2016). Tillage practices are wellsprings of the high rate of disintegration on account of the land cover change. Catchments are sensitive to land use dynamics induced by human activities. Land cover changes are predicted to have an important effect on river flows and sediment yields from a catchment. Hydrological response dynamics (an integrated indicator of watershed conditions) and water response in different river basins are affected by changes in land use and climate. Land use activities, development, and management of water resource are interdependent. Sedimentation in water resources is the outcome of the land erosion in its

catchment area. Land erosion fundamentally has an impact on physical and chemical characteristics of soils and causes on-site nutrient loss and off-site sedimentation and nutrients enrichment of water resources (Sewnet, 2015).

To categorize, prioritize and compare watersheds those that are sensitive to change and to help management attempts to minimize undesired effects requires, enhanced assessment and understanding of the relationship among environment change, land use change, runoff and water quality at the landscape measure (Joseck et al., 2016). The watershed process is highly dynamic in both space and time. Overall statements about land-water interactions need to be constantly questioned to determine whether they represent the best available information which supports decision making processes for developmental actions in a maintainable way (Sayemuzzaman and Jha, 2014). Local-scale hydrological models and GIS can play a dynamic role in river basin monitoring. They simulate influences on possible future changes of LULC and help to find measures refining adaptive capability of river basins. The growth of agriculture, urbanization, deforestation and the day to day activities of human beings has resulted to progressive and spatial change in land use and land cover which have affected water flow pathways and water balance (Chhabra et al., 2006).

Developing countries like Ethiopia, where agriculture serves as the backbone of the economy, are adversely affected by land use and land cover change. Besides these problems, various water resource development sectors (hydropower, irrigation, urban and rural water supply) have persistently been affected by both temporal and spatial changes of LULC (Nigussie and Yared, 2010).Today, runoff and soil erosion in catchment areas and its subsequent deposition in rivers, lakes, and reservoirs are of the great worry to humanity(Wilson and Weng, 2011) .

Dabus catchment is facing high soil erosion from the effects of intense rainfall which aggravates the land cover change. This continuous change in land cover has influenced the water balance of the watershed by changing the magnitude and pattern of the components of stream flow. These components include surface runoff and groundwater flow, whose results and effects increase the extent of water management problem. Moreover, this examination additionally points estimation of residue yield under various land use/land spread changes for the long stretches of 1986, 2019 and 2029 utilizing SWAT.

2. Materials and Methods

2.1 Description of the Study Area

This study was conducted in Dabus sub-catchment and its encompassing environs in Southwestern Ethiopia. The area is located between longitudes 34°30′0″E and 34°45′0″ E and latitudes 9°30′0″N and 9°45′0″ N (Fig. 3.1).

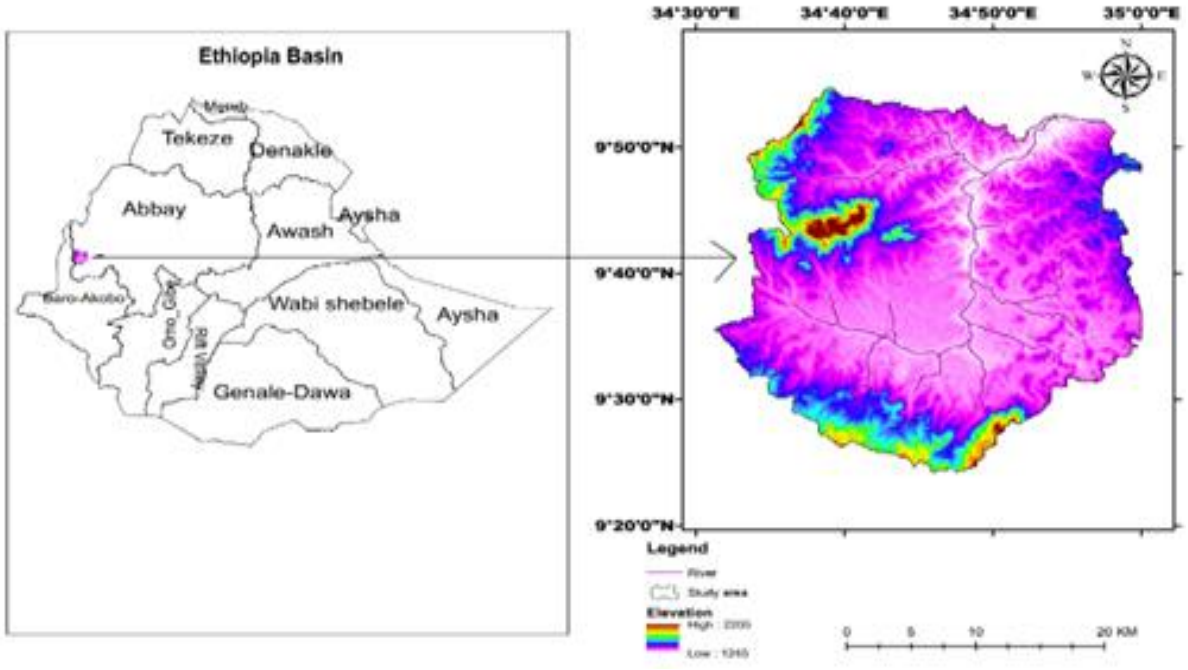

Fig. 3.1: Location of the Dabus Catchment in Ethiopia.

The normal temperature and precipitation are about 21.9°C and 1222 mm, respectively. Most of the territory portrayed by a semiarid atmosphere with moderate precipitation and the greater part of the absolute yearly precipitation is gotten during one blustery season (June to September). The study zone comprises 3 regions, in particular Bambasi, selga and Bagi. Dabus sub-catchment largely occurs in Benshangule gumze provincial state and partly in Oromya territorial state. It is tremendously expanded catchment as far as geology, atmosphere land use and socio-financial matters. The normal elevation is 2097 m with a mean slant of 12.31%. There is high fleeting variety as opposed to spatial variety of precipitation in the examination territory. It has high diurnal change in temperature for example there is high variability between the day by day most extreme and least temperature to a normal temperature of 21°C. The Dabus River alone contributes 13% and 22% of the all-out yearly progression of the abay water during the dry an flood season separately (Degefu, 2003).

2.2 Analyze surface runoff and sediment for the past and future scenarios

2.2.1 SWAT model and inputs

SWAT is a semi-distributed and physically based watershed model that operates on a continuous time-step (Tuppad et al., 2010). The model is designed to simulate the effects of changes in the catchment management practices on surface water and groundwater hydrology, diffuse pollution and sediment erosion within catchments (KNMI, 2000). Two kinds of data; spatial data and temporal data are required by SWAT model. Spatial data include a digital elevation model (DEM), land-use map and soil map. The temporary data include hydrological data (stream flow & sediment yield) and climatic data (precipitation, solar radiation, relative humidity, wind speed and temperature). Within SWAT, a catchment is divided into multiple sub-catchments which are then further divided into Hydrologic Response Units (HRUs) that consist of homogeneous land use, slope and soil characteristics. The simulation processes of watershed using SWAT are split into two phases: as (i) land- based phase and (ii) Routing phase (channel-based phase) (Rao, 2015). The land-based phase controls the loadings like runoff, sediment, nutrient and pesticides. While, the channel based flights the loadings throughout the stream network (Srinivasan et al., 2012).

2.2.2 Hydro-meteorological data

The long-term records (1986−2014) meteorological data were collected from four stations which lie inside the boarder of the study area. The observations of meteorological variables of each station were obtained from National Meteorological Stations of Ethiopia. Since relative humidity, wind speed and solar radiation data records were limited for all the stations except for the Asosa, bako and Bambasi stations weather generator capabilities of SWAT model was used to generate this data by using bagie station records. Daily stream flow records (1986–2006) at Bagie gauging station was obtained from the hydrology department of Ministry of Water Resource, Irrigation and Energy of Ethiopia (MWRIEE). The sediment concentration record has been a challenge to obtain since measurements on sediment concentration taken by the MWRIEE is in a noncontiguous time step. Hence the sediment data was prepared through a sediment rating curve using a series data record for 100 days in 2005 and 2006 at Dabus sub-catchment site from MWRIEE.

2.2.3 Geographical or spatial datasets

The digital elevation model (DEM) of Dabus sub-catchment (Fig. 3.4) was obtained by downloading from ASTER GDEM website http://gdem.ersdac.jspacesystems.or.jp/ with 30 by 30 m DEM resolution. This DEM was used to delineate the catchment and the drainage patterns of the surface area analysis. Sub basin parameters such as slope length of the terrain, slope gradient and the stream network characteristics such as channel length, slope, and width were derived from this DEM. It was also used to determine the hydrological parameters of the catchment such as flow accumulation, direction, and stream network (Besalatpour et al., 2012).

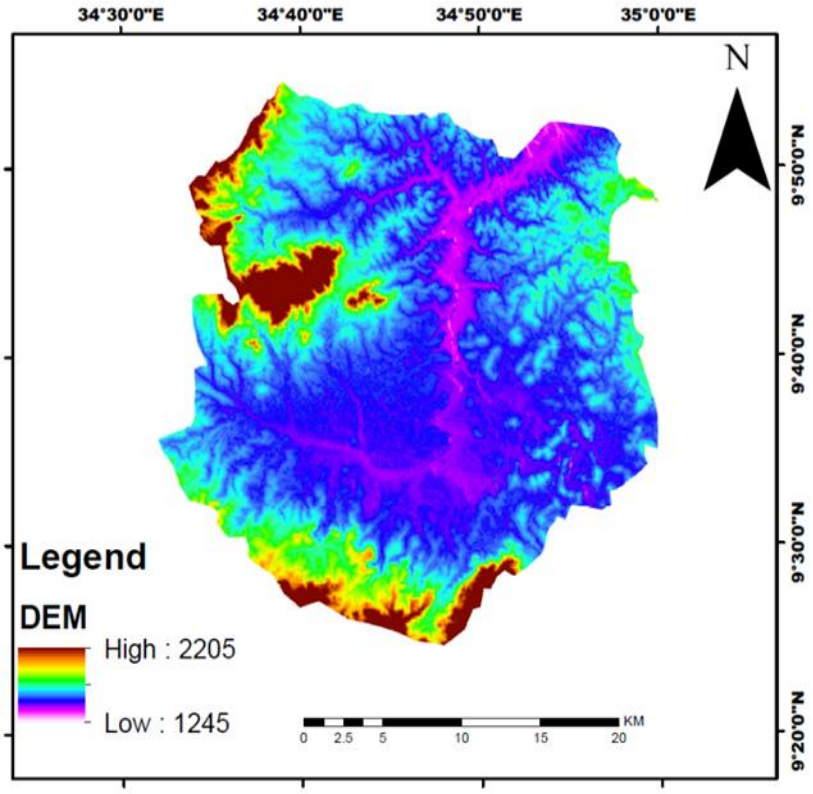

Fig. 3.2: Digital elevation model of Dabus sub-catchment.

A digitized soil map of Dabus sub-catchment was obtained from the Ministry of Agriculture of Ethiopia in the form of shape file. The map of soil types within the sub-catchment was then derived from this National Soil Map vector dataset. The shape file was converted in to grid format using Arc GIS 10.5 as shown in Fig. 3.5.

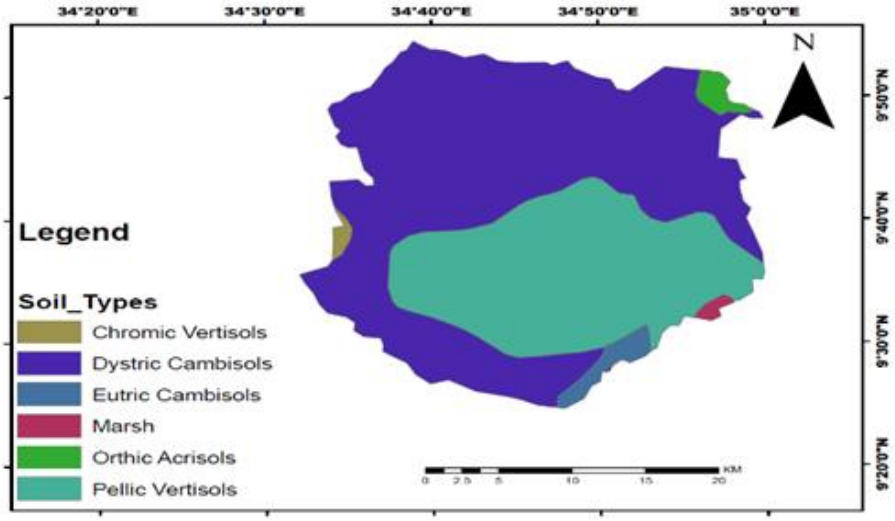

Fig. 3.3: Soil map of Dabus sub-catchment.

The soil data were used to determine the needed into physical and chemical characteristics of the soil, which both play a large role in determining the movement of water and air within the HRU. The properties required by SWAT for each layer of each soil type include the depth of the soil layer, soil texture, hydraulic conductivity, bulk density and organic carbon content and soil depth for the different layers of soil were obtained mainly from Dabus River basin integrated development master plan and major soils of the world (FAO, 2011).

The digital land use/ land cover data of the study area was obtained the past LULC variation information of 1986–1993, 1993–2019, and 1986–2019 were utilized as a benchmark of the historical LULC. After that, the Markov model was used to produce the transition area file. The CA_Markov model was then applied to forecast the 2029 LULC condition using the Tersest Geospatial Modeling and Monitoring System software Figure 3.6.

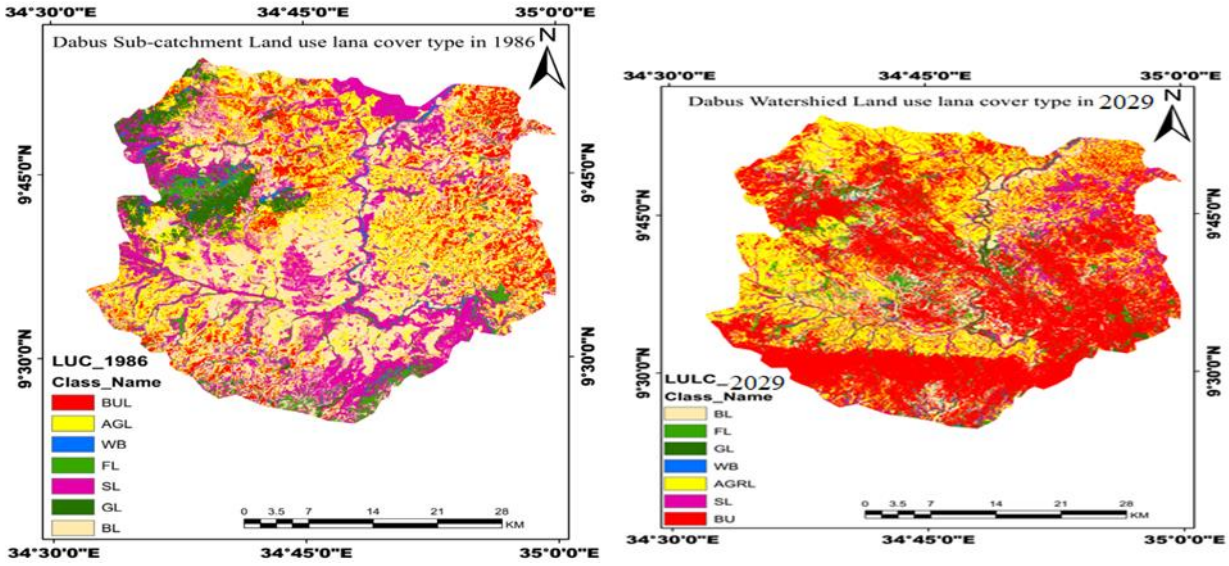

(a) (b)

Fig. 3.4: Historical LULC map (a) (1986 LULC) and Predicted LULC map (b) (2029).

2.3 SWAT model simulation, sensitivity analysis, calibration and validation

SWAT input parameters are process based and must be held within the realistic uncertainty range. Because the default simulation outputs in SWAT model run can't be directly used for further analysis. Instead, the ability of the model to sufficiently predict the constituent stream flow and sediment yield should be evaluated through sensitivity analysis, model calibration and validation steps.

2.3.1 Sensitivity analysis

Performing calibration process for all model parameters of flow and sediment yield is computationally far-reaching and complex. Hence, sensitivity analysis for the SWAT model set up is important as parameter sensitivity analysis provides insights to which parameters contribute most to the output variance due to input variability (Li et al., 2009). Therefore, the vital aspect of parameter sensitivity analysis is to allow the possible reduction in the number of parameters that must be estimated, thereby reducing the computational time required for model calibration. In this study, sensitivity analysis was performed for each flow and sediment parameter within its allowable range was approximated using the relative sensitivity index shown in Equation 3.19 (Agoyi et al., 2014).

$$S_r = (\frac{X}{Y})(\frac{y_2 - y_1}{x_1 - x_2}) \quad (3.1)$$

Where:

S_r = is the relative sensitivity index,
X =is the parameter and
y =is the predicted output.
x_1, x_2 and y1, y_2 correspond to ±10 percent of the initial parameter and corresponding output
values, respectively (Besalatpour et al. 2012).
The greater the Sr, the more sensitive a model output variable was to that particular parameter. However, it has some limitations using relative sensitivity index (S_r) to assess parameters within a model. Primarily, these limitations are related to the assumption of linearity, the lack of consideration to correlations between parameters, and the lack of consideration to the different degrees of uncertainty associated with each parameter. Sensitivity analysis can generally be performed by changing value one at a time (Local) or allowing all parameter values to change (Global) (Lenhart et al., 2002).
Both methods have their own disadvantage. The problems with one at a time analysis is the correct value of other parameters that are fixed are never known. Because sensitivity of one parameter often depends on the value of other parameters. The disadvantage of Global sensitivity analysis is that it needs a large number of simulations. Both producers however provide insight in to the sensitivity of the parameter and are necessary steps in model calibration. Unfortunately, the sensitivity analysis method implemented in SWAT model is called the Latin hypercube One At- a – Time (LH-OAT) design as proposed by Lenhart et al. (2002).This type of sensitivity analysis combines the strength of global and local sensitivity analysis methods (Lenhart et al., 2002). The LH-OAT performs LH sampling followed by OAT sampling. LH sampling uses stratified sampling approach that better covers a sampling hypercube with fewer samples. In this study stream flow sensitivity analysis followed by sediment yield analysis was performed for each time reference land uses (1986 LULC and 2029 LULC). The sensitivity of parameters was categorized in to classes of small to 0 < RS < 0.05, Medium (0.05 < RS<0.2, High 0.2<RS<1, very high RS > 1.0 according to Lenhart et al. (2002). The detailed definition and ranges of parameters was dictated and analyses of the most sensitive parameters were selected and their sensitivity was ranked in a way that parameter ranked 1 was considered the most sensitive. Accordingly, both flow and sediment parameters were selected for calibration those their value ranges between very high to medium classes of sensitivity class above.

2.3.2 Model calibration, evaluation and validation methods

Before calibration proceeds the performance of the model was evaluated for the initial simulation with the model default parameter values. But the default SWAT simulation result was with inconsistency between measured and simulated outputs (Besalatpour et al., 2012). Hence both automatic and manual calibrations were done respectively. SWAT model calibration for stream flow and sediment yield were performed for 1986 LULC and 2029 LULC separately at the watershed outlet (Welde and Gebremariam, 2017). Only sensitive parameters were included in the calibration of the model at a monthly time-step against observations of discharge and sediment yield loads recorded at the outlet of the Dabus sub-catchment.
After running of the model for analysis of results, simulated stream flow and sediment yield were evaluated by visual inspection and quantitative statistics i.e. to evaluate how the model simulates well. For quantitative statistics the model performance was evaluated using three statistical criteria, the coefficient of determination (R^2), Nash- Sutcliffe efficiency (NSE) and percent bias (PBIAS) as recommended by Moriasi et al. (2007). NSE is a normalized statistic that describes the relative magnitude of the residual variance as compared to the observed and demonstrates how well the plot of observed versus the simulated value fits the 1:1 line. The Nash-Sutcliffe Efficiency (NSE) coefficient proposed by Welde and Gebremariam (2017) is defined by Equation (3.21) (Welde & Gebremariam, 2017). R^2 ranges from 0 to 1 and explains the proportion of variance in the observed data with higher values indicating less error variance. R^2 is defined by Equation (3.20). PBIAS measures the average tendency of the simulated data to be larger or smaller than their observed counterparts and is defined by Equation (3.22). A positive value PBIAS indicates model underestimation bias and negative value indicates model over estimation bias. In general model simulation can be judged as satisfactory if NSE > 0.4 and R^2 > 0.5 and PBIAS ± 25% for stream flow and PBIAS ± 55% for sediment yield (Singh et al., 2014).
Model validation was done to ensure that the calibrated set of parameters performs reasonably well under an independent data set. In order to utilize any predictive watershed model for estimating the effectiveness of feature potential management practices the model was validated against an independent dataset without adjusting calibrated parameters. The period of 1986–1988 and 2005–2008 daily stream flow and sediment yield data were used for model validation of selected flow and sediment parameters for 1986 and 2029 LULC respectively in monthly time scale and general framework of the methodology used presented in Figure 3.7.

$$R^2 = \frac{\sum_{i=1}^{n}(Y_{obs} - \bar{Y}_{obs})(Y_{sim} - \bar{Y}_{sim})}{\sqrt{\sum_{1}^{n}(Y_{obs} - \bar{Y}_{obs})2}\sqrt{\sum_{1}^{n}(Y_{sim} - \bar{Y}_{sim})2}} \quad (3.2)$$

$$NSE = 1 - \left[\frac{\sum_{i=1}^{n}(Y_{obs} - Y_{sim})^2}{\sum_{i=1}^{n}(Y_{obs} - \bar{Y}_{obs})^2}\right] \quad (3.3)$$

$$PBIAS = \frac{\sum_{i=1}^{n}(Y_{obs} - Y_{sim})}{\sum_{i=1}^{n}Y_{obs}} * 100\,\% \quad (3.4)$$

Where:

Y_{sim} and Y_{obs} = are the simulated and observed values respectively,
Y_{obs} = is the mean of n observed values; and
Y_{sim} = is the mean of n simulated values (Welde and Gebremariam, 2017).

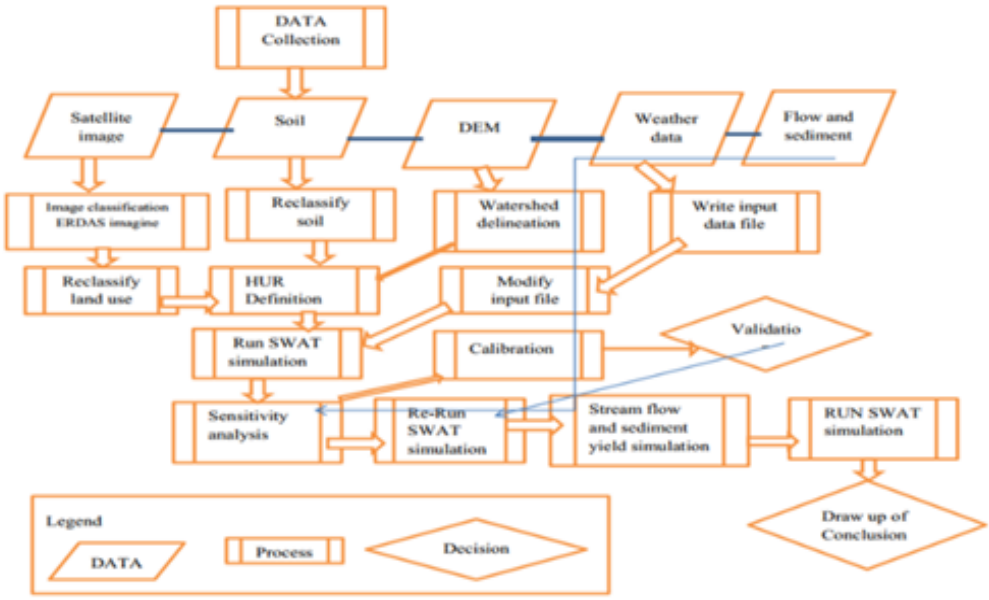

Fig. 3.5: General Framework of the study.

3. Result and Discution

3.1 Analysis of surface runoff and sediment for the past and future scenarios

3.1.1 Sensitivity analysis and parameters calibration

Sensitivity examination outcomes of SWAT model stream flow limits are recognized as important for a period of five years (1986−1991) and seven years (1996−2002). It shows a range of small to high sensitivity class for 1986 LULC and 2029 LULC respectively. As shown in Table 4.9, the upper three sensitive flow limits have the same rank and sensitivity class for both LULC orientation years. The difference in sensitivity level of flow limits for the two reference land uses occurs for those parameters which their sensitivity index lies between the medium and low classes. Practically, comparable outcomes are also reported by Neuroimaging et al. (2010). The authors found that, depending on the sensitivity index, eight and ten flow parameters which had their index value ranging between medium and high for 1986 and 2029 LULC respectively were selected for calibration.

Table 4.9: Flow parameter sensitivity analysis result for 1986 LULC.

SWAT code	Flow parameter description	RS	Rank	Sensitivity class
CN2	Initial SCS CN II value (%)	0.462	1	High
ALPHA_BF	Alpha base flow recession constant (days)	0.411	2	High
GWQMN	Threshold depth of water required for return flow to occur			
		0.289	3	High
SOL_Z	Soil depth (mm)	0.157	4	Medium
ESCO	Soil evaporation compensation factor	0.146	5	Medium
SOL_AWC	Available water capacity (mm of water/mm soil)	0.140	6	Medium
BLAI	Maximum potential leaf area index	0.074	7	Medium
CANMX	Maximum canopy index	0.068	8	Medium
REVAPMN	Threshold depth of water required for return Re-evaporation to occur (mm)			
		0.058	9	Medium
CH_K2	Effective channel hydraulic conductivity (mm/hr)	0.047	10	Medium
GW_REVAP	Ground water re-evaporation coefficient	0.041	11	Small
EPCO	Plant evaporation compensation factor	0.038	12	Small
SOL_K	Soil conductivity (mm/hr)	0.027	13	Small
Slope	Average slope steepness (m/m)	0.018	14	Small
GW_DELAY	Ground water delay (day)	0.016	15	Small
CH_N2	Manning coefficient for channel	0.009	16	Small

Note: RS, is relative sensitivity: small to negligible 0 < RS < 0.05, Medium (0.05 < RS<0.2, High 0.2<RS<1, very high RS > 1.0,

The initial curve number II, the parameter which is related to runoff as a function of soil permeability, land use and antecedent soil water conditions, and was the most sensitive of all. This was followed by Alpha base factor (Alpha_Bf), which is a direct index of the groundwater flow response to changes in recharges. The threshold depth of water in the shallow aquifer required for the flow to occur (GWQMN) was the third most sensitive parameter. The top three sensitive flow parameters were the same for both 1986 LULC and 2029 LULC. The variation in sensitivity of flow parameters for the two-reference land use occurred for those parameters which had their

sensitivity index fall in the medium sensitivity class.

Flow parameters which were moderately sensitive for 1986 LULC were soil layer depth from the soil surface to the bottom of the layer (SOL_Z), soil evaporation compensation factor (ESCO) and the allowable water capacity of the soil layer among the soil properties of the watershed. The flow was also moderately sensitive to crop parameters: maximum potential leaf area index (BLAI), which is a parameter to quantify the density of the plant and the maximum canopy storage (CANMX), which indicates the maximum amount of water that can be trapped in the canopy on a given day.

Similar to the 1986 LULC in Dabus watershed, 2029 LULC was also moderately sensitive to soil parameters (ESCO, SOIL_AWC, SOIL_Z), crop parameters (BLAI, EPCO), Effective channel hydraulic conductivity (Ch_K2) and Ground water "revap" coefficient, but their value of sensitivity and rank varied as compared to 1986 LULC (Table 4.9 and 4.10). GWQMN and GW_REVAP have an effect on the volume of groundwater flow and govern the upsurge of groundwater into the unsaturated soil zone. The effects of these parameters on base flow also affect runoff, and low values of GWQMN correspond to high runoff (Gull et al., 2017).

Table 4.10: flow parameter sensitivity analysis result for 2029 LULC.

SWAT code	Flow parameter description	RS	Rank	Sensitivity class
CN2	Initial SCS CN II value (%)	0.6600	1	High
Alpha_Bf	Alpha base flow recession constant (days)	0.4700	2	High
Gwqmn	Threshold depth of water required for return flow to occur	0.3500	3	High
Esco	Soil evaporation compensation factor	0.2800	4	High
Sol_Awc	Available water capacity (mm of water/mm soil	0.2000	5	Medium
Sol_Z	Soil depth (mm)	0.1500	6	Medium
Blai	Maximum potential leaf area index	0.0700	7	Medium
Soil_K	Soil conductivity (mm/hr)	0.0500	8	Medium
Gw_Revap	Ground water revaporation coefficient	0.0570	9	Medium
Epco	Plant evaporation compensation factor	0.0450	10	Medium
Canmx	Maximum canopy storage	0.0456	11	Medium
Revapmn	Threshold depth of water required for return revaporation to occur (mm)	0.0263	12	Small
Ch_K2	Effective channel hydraulic conductivity (mm/hr)	0.0190	14	Small
Epco	Plant evaporation compensation factor	0.0180	15	Small
Ch_N2	Manning coefficient for main channel	0.0130	16	Small
Slope	Average slope steepness (m/m)	0.0052	17	Small
Gw_Delay	Ground water delay (day)	0.0043	18	Small
Sol_Alb	Soil Albedo	0.0034	19	Small

The initial simulation using the default values was unable to appropriately reproduce the runoff in the sub-basin because the actual discharge peaks were overestimated and the base flow was underestimated. Consequently, parameter calibration was desirable after identifying the most sensitive parameters for runoff shown in Table 4.11.

Table 4.11: Calibrated flow Parameters.

		1986			**2029**	
Rank	Parameter	Allowable range	Calibrated value	Parameter	Allowable range	Calibrated value
1	CN2	0–100	−15.00%	CN2	0 −100	−14.5%
2	ALPHA_BF	0–1	0.80	ALPHA_BF	0–1	0.7
3	GWQMN	0–5000	2700.00	GWQMN	0–5000	3120
4	SOL_Z	0–3000	8.00%	ESCO	0–1	0.7
5	ESCO	0.01–1	0.70	SOL_AWC	0–1	−5.5
6	SOL_AWC	0–1	3.50%	SOL_Z	0–3000	6.4%
7	BLAI	0–1	0.10	BLAI	0–1	0.1
8	CANMX	0–10	0.05	SOL_K	0–100	18%

The periods 1986 – 1991 and 1996 – 2002 were used for stream calibration of 1986 LULC and 2029 LULC respectively. These periods were selected for model calibration as meteorological and stream flow records were complete and included both high and low flow conditions comparatively. The CN2 was decreased by 15% and 14.5% for 1986 and 2029 respectively, of the original value to decrease the runoff and increase infiltration. SOL_AWC was increased by 3.5% in 1986 to reduce the movement of water within the soil. However, for 2029, SOL_AWC was decreased by 5.5% to increase the movement of water within the soil profile. For 2029, the value of SOL_K resulted in an underestimation of the lateral flow in the study area. Hence, the SOL_K was increased by 18% to increase the lateral flow within the soil. For the simulated runoff to become closer to the observed runoff, the ESCO value was adjusted to 0.7 for both 1986 and 2019.

Flow hydrographs were generated to compare observed and simulated flow values for the calibration periods of each LULC in monthly time scale (Figs. 4.6 and 4.7). Both the calibration and validation periods indicated that the model achieved a relatively good fit between predictions and observations.

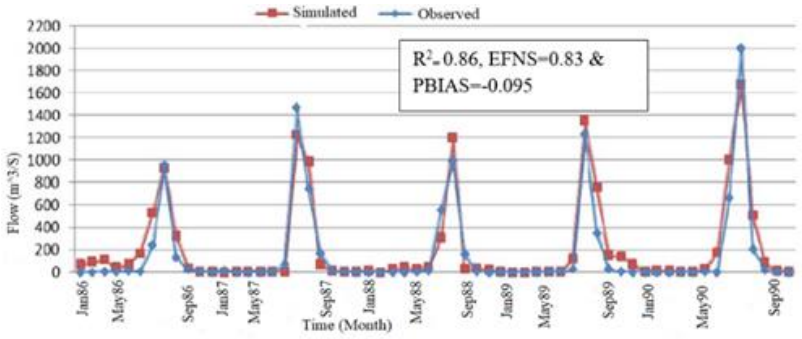

Fig. 4.6: Observed and simulated monthly flow of calibration for 1986 LULC.

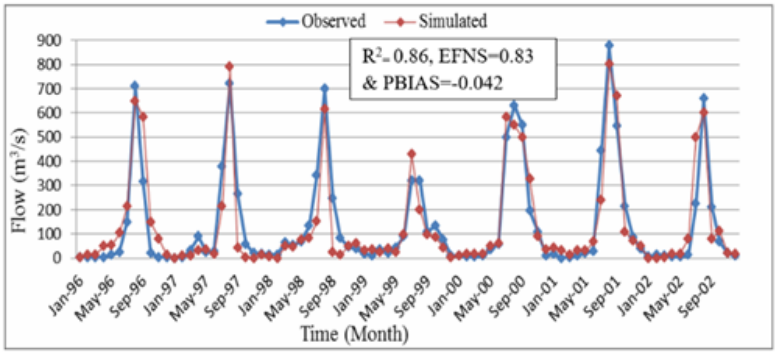

Fig. 4.7: Observed and simulated monthly flow of calibration for 2029 LULC.

The simulated flow value for both 1986 LULC and 2029 LULC were slightly less than that of the measured value at peak flow months (August). However, the simulated flow is slightly higher than the measured value at low flow months (January to May). Generally, the model slightly overestimates mean monthly stream flow for each specified land use reference years.

The monthly flow observed and simulated results for validation periods of 1986 LULC and 2029 LULC is presented in Fig. 4.8 and 4.9. During the validation period (1993 – 1995) & (2003 -2006) for 1986 LULC and 2029 LULC respectively, the performance of the model was evaluated using performance indicators. For 1986 LULC the model showed good performance with 85.02%, 86.58% and -6.74% of R^2, ENS and PBIAS respectively. Whereas, the values of R^2, ENS and PBIAS were 84.5%, 80.32% and -9.55% respectively for 2029 LULC.

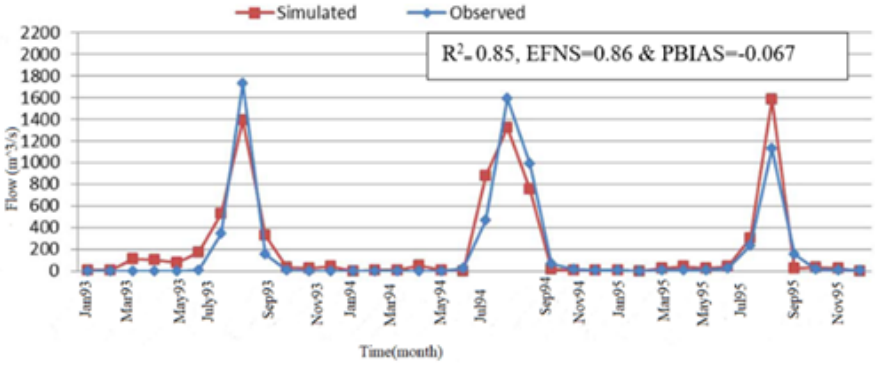

Figure 4.8: Observed and simulate monthly flow of validation for 1986 LULC.

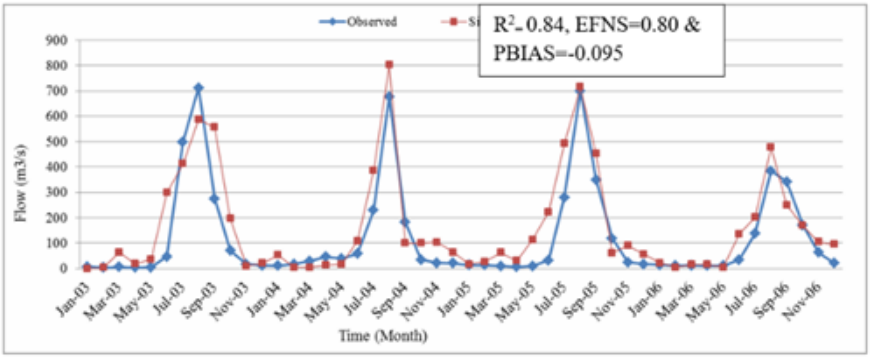

Fig. 4.9: Observed and simulate monthly flow of validation for 2029 LULC.

The model performance indicators; correlation coefficient (R^2), Nash-Sutcliffe simulation efficiency (ENS) and percent bias (PBIAS) were summarized in Table 4.12. The model stream flow simulation provides confidence for the further application of the model to assess stream flow hydrologic response analysis caused by spatial and temporal variability of the watershed characteristics. Observed flow data during calibration and validation periods, indicated that the model achieved a relatively good fit between predictions and observations.

Table 4.12: Calibration and validation statistics of simulated and observed monthly flow.

Parameters	1986 LULC		2029 LULC	
	Calibration (1986-1996)	Validation (1986-1996)	Calibration (1996-2002)	Validation (2003-2006)
R^2	0.860	0.850	0.860	0.840
ENS	0.830	0.860	0.830	0.800
PBIAS	-0.095	-0.067	-0.042	-0.095
Time Step	Monthly	Monthly	Monthly	Monthly

3.1.2 Evaluation of Sediment yield

Model sediment parameter analysis for Dabus watershed was done at the outlet sub basin (sub basin 1) through 240 iterations (12 parameters * 20 iteration per parameter) for each LULC map. Ten out of 12 analyzed SWAT sediment flow parameters that directly govern the sediment yield and transport in the watershed were found to be sensitive for 1986 land uses (Table 4.13) but 11 parameters were found to be sensitive for 2008 LULC (Table 4.14). It should be noted that these parameters can be categorized into two groups as upland and channel factors. The former group includes parameters such as USLE_P, USLE_C, USLE_K and BIOMIX, whereas, SPEXP, SPCON and CH_COV parameters belong to the latter group. Similar result were also found by Mengistu & Sorteberg (2012) [USL_P (0.872), SPCON (0.853), and SPCON (0.58)].

Table 4.13: Sediment parameters sensitivity analysis result for 1986 LULC.

SWAT_code	Sediment parameter name	RS	Rank	Class
USL_P	USLE support practice factor	0.8620	1	High
SPCON	Linear factor for channel sediment routing	0.8520	2	High
SLOPE	Average slope steepness (mm/mm)	0.5670	3	High
SOL-AWC	Available water capacity (mm H_2O/mm soil	0.2750	4	Medium
SPEXP	Exponential factor for sediment routing	0.0670	5	Medium
SOL_K	Soil conductivity (mm/hr)	0.0570	6	Medium
BLAI	Maximum potential leaf area index	0.0455	7	Small
USLE_C	USLE cover factor	0.0344	8	Small
SOL_ALB	Soil albedo	0.0147	9	Small
CH_EROD	Chanel erodibility factor	0.0166	10	Small

Note: RS, is relative sensitivity: small to negligible 0 < RS < 0.05, Medium 0.05 < RS<0.2, High 0.2<RS<1, very high RS > 1.0

The high-class sensitive sediment parameters are the same for both 1986 LULC and 2029 LULC including their rank. On the other hand, for the medium and lower sensitive parameters, their rank and class of sensitivity were interchanged for 2029 LULC as shown in Table 4.14

Table 4.14: Sediment parameters sensitivity analysis result for 2029 LULC.

SWAT_code	Sediment parameter name	RS	Rank	Class
USL_P	USLE support practice factor	0.866	1	High
SPCON	Linear factor for channel sediment routing	0.755	2	High
SLOPE	Average slope steepness (mm/mm)	0.600	3	High
CH_COV	Chanel cover factor	0.267	4	Medium
SOL_AWC	Available water capacity (mm H_2O/mm soil	0.057	5	Medium
SOL_K	Soil conductivity (mm/hr)	0.047	6	Medium
SPEXP	Exponential factor for sediment routing	0.024	7	Small
USLE_C	USLE cover factor	0.029	8	Small
USLE_K	USLE soil erodibility	0.016	9	Small
BLAI	Maximum potential leaf area index	0.010	10	Small
SOL_ALB	Soil Albido	0.011	11	small

Note: RS, is relative sensitivity: small to negligible 0 < RS < 0.05, Medium (0.05 < RS<0.2, High 0.2<RS<1, very high RS > 1.

From Table 4.14, seven and eight parameters for 1986 and 2029 LULC respectively were selected according to their sensitivity index which had their class of sensitivity ranging from high to medium class for calibration. Table 4.13 and 4.14 indicate that same channel factors (SPCON and CH_COV) were more sensitive than same upland parameters (soil erodibility and initial residue cover). These rankings are not surprising to the author because, the analysis of sediment flow data indicates that sediment loads though low in magnitudes are sustained even during the dry

days.

The following final sediment parameter values (Table 4.15 and 4.16) were accepted after respective modification and adjustment of the default/initial values. For example, the USLE support practice (USLE_P) which is the ratio of the soil loss with the specific support practice to the corresponding loss with up and down slope culture were adjusted to 0.78 and 0.76 for 1986 LULC and 2029 LULC respectively from highly sensitive class sediment parameters of the watershed. The linear parameter for calculating the maximum amount of sediment that can be re-entered during sediment routing (SPCON) were adjusted to 0.0093 and 0.0056 for 1986 LULC and 2029 LULC respectively.

Table 4.15: Calibrated sediment Parameters for 1986 LULC.

Rank	Parameter	Allowable range	Effect on simulation when parameter value Increase	Calibrated value
1	USL_P	0-1	Reduce soil erosion & surface runoff	0.7800
2	SPCON	0.0001-0.01	Increase concentration of sediment that can transport by the water	0.0093
3	SLOPE	0-1	Decrease base flow	+6.000%
4	SOL-AWC	0-1	Decrease surface runoff	+9.00%
5	SPEXP	1-2	Increase concentration of sediment that can transport by the water	2.340
6	SOL_K	0-100	Increase ground water flow & decrease surface Runoff	45.000
7	BIOMIX	0-1	Decrease surface runoff & erosion	0.080

All the sensitive sediment parameters for 1986 LULC were calibrated for 2029 LULC with an additional parameter (USLE_C) as shown in Table 4.16.

Table 4.16: Calibrated sediment Parameters for 2029 LULC.

Rank	Parameter	Allowable range	Effect on simulation when parameter value Increase	Calibrated value
1	USL_P	0-1	Reduce soil erosion & surface runoff	0.7600
2	Spcon	0.0001-0.01	Increase concentration of sediment that can transport by the water	0.0056
3	Slope	0-1	Increase erosive power of flow	+5.5000%
4	Ch_Cov	0-1	Increase erosion from bed and banks of channel	0.62
5	Sol_AWC	0-1	Decrease surface runoff	+8.00%
6	SOL_K	0-100	Increase ground water flow & decrease surface Runoff	55.70
7	Spexp	1-2	Increase concentration of sediment that can transport by the water	1.25
8	USLE_C	0-1	Decrease soil erosion	0.30

The ratio of soil loss from agricultural land under specific conditions to the corresponding losses from bare land, called the USLE cover and management factor (USLE_C). This is the factor that measures the combined effect of all the interrelated cover and management variables. SWAT calculates the actual C factor based on the amount of soil cover and minimum C factor defined for the plan/land cover. The minimum C factor quantifies the maximum decrease in erosion possible for the plan/land cover. Since the USLE C factor is influenced by management, this variable has to be adjusted by the user to reflect management conditions in a watershed of interest.

Accordingly, USLE_C factor was modified to 0.3 for 1986 LULC. Following the adjustment of the default values of sediment parameters (upland and channel factors), statistical model performance indicators (R^2, NSE and PBIAS) were used for evaluating the model prediction efficiency. Accordingly, presented in Table 4.17, coefficient of determination (R^2), Nash – Sutcliffe coefficient (NSE) and percent bias were 88.02%, 87.45% and -5.66% respectively for 1986 LULC and 86.33%, 88.75% and -9.41% for 2029 LULC. All values of the Statistical indicators are above the lower acceptable limit. This shows that the model performed well in sediment calibration. Hence the objective function was obtained.

Table 4.17: Sediment yield Calibration and validation model performance statistics.

	1986 LULC			2029 LULC	
Parameters	**Calibration (1986-1991)**	**Validation (1993-1995)**		**Calibration (1996-2002)**	**Validation (2003-2006)**
R2	0.88	0.83		0.86	0.82
ENS	0.87	0.82		0.88	0.84
PBIAS	-0.0566	-0.0675		-0.0941	-0.0765
Time step	**Monthly**	**Monthly**		**Monthly**	**Monthly**

Monthly time setup for sediment yield hydrograph was generated to compare the observed and simulated sediment load values for the calibration period (1986– 1991) Figure 4.10 and (1996- 2002) Figure 4.11 fors 1986 LULC and 2029 LULC, respectively.

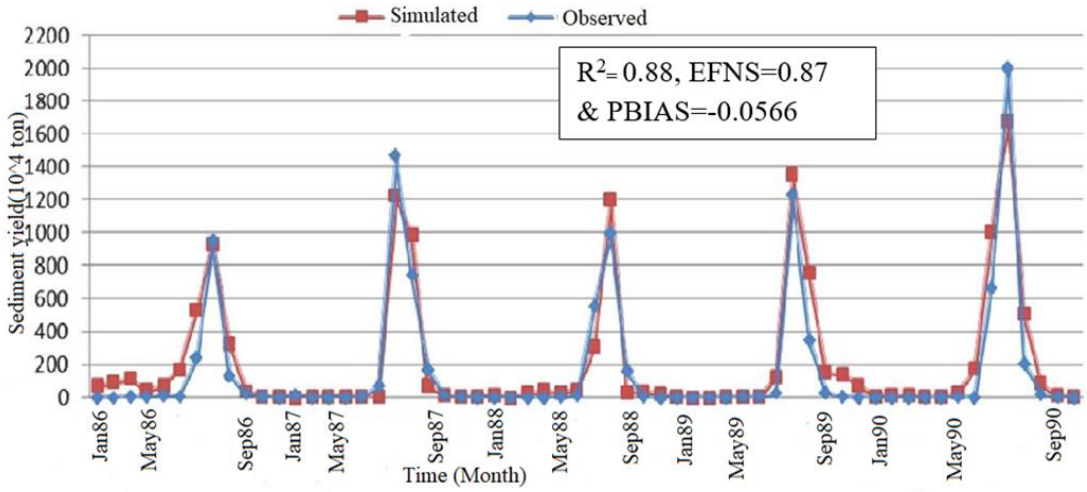

Fig. 4.10: Observed and simulated monthly sediment yield calibration for 1986 LULC

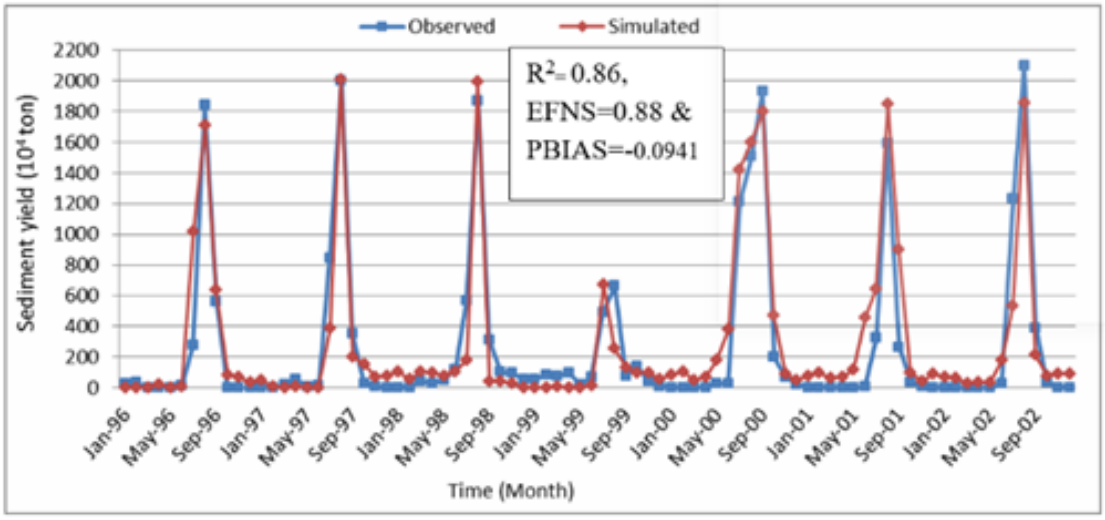

Fig. 4.11: Observed and simulated monthly sediment yield calibration for 2029 LULC

As shown in Figures 4.10 and 4.11, the monthly simulated sediment yield was overestimated for both LULC reference times (1986LULC & 2029 LULC). Comparatively, the model overestimated the results of 2029 LULC of low sediment seasons as compared to 1986 LULC. For the medium and high sediment yield seasons, the model estimated better than for 1986 LULC.

3.1.3 Sediment yield Validation

The sediment yield hydrograph for the calibration period was validated using independent data set of observed sediment yield without adjusting calibrated sediment parameters for each land use and land cover reference years. Similar to the calibration period, the sediment yield hydrograph of measured and simulated output for the monthly time setup during the validation period (1993-1995) for 1986 LULC & (2003-2006) for 2029 LULC showed good agreement for both reference land uses as shown in Figure 4.12 and 4.13.

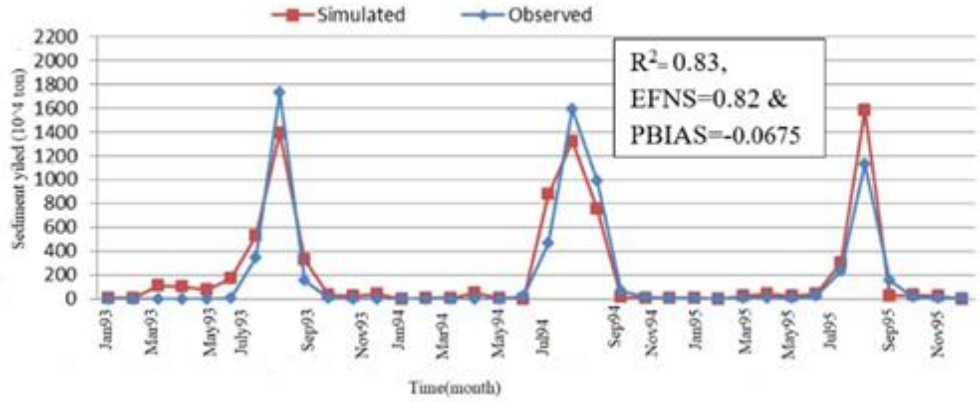

Fig. 4.12: Observed and simulated monthly sediment yield validation for 1986 LULC.

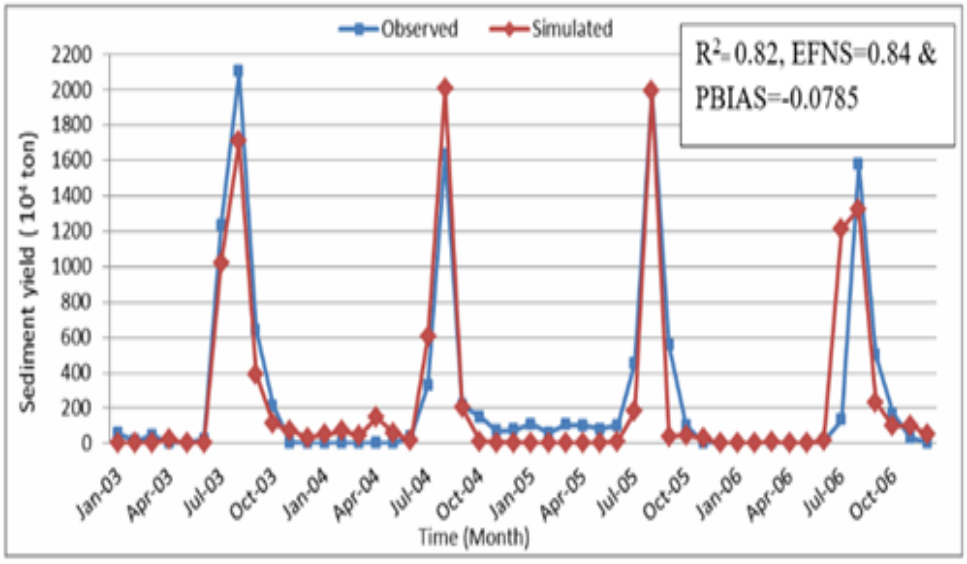

Fig. 4.13: Observed and simulated monthly sediment yield validation for 2029 LULC.

3.2 Modeling stream flow and sediment yield response to land use dynamics

3.2.1 Establishing scenarios for assessing impacts of LULC change

The weather data sets were separated into two periods, 1986 – 1997 (representing the 1990s) and 1997- 2008 (representing 2001s). The land use maps of 1986 and 2029 were used to reflect the land use pattern for the 1990s and 2002s respectively. As a result, three scenarios were established as follows.

8 **Scenario (I)**: Weather of the 2001s and LULC of 2029 (future LULC)

9 **Scenario (II)**: weather of the 2002s and LULC of 1986 (paste LULC)

10 **Scenario (III)**: weather of the 1995s and LULC of 1986 (LULC and weathers)

Simulation was performed for each scenario. The Scenario I and scenario III were simulated using the calibrated parameters of each land use. But scenario II was simulated without changing the calibrated parameters of 1986 land use land cover. Hence simulation were done for scenario I and scenario II for the period of 1996 – 2009 using 2029LULC and 1986 LULC respectively. Whereas, scenario III was simulated for the period of 1986 – 1996 using 1986 LULC (Table 4.18).

Table 4.18: LULC of Dabus sub-catchment for scenario I (2029) and scenario II (1986).

SWAT Code	LULC Types	1986		2029		LULC TYPES CHANGE 1986 - 2029	
		Area in Km²	%	Area in Km²	%	Area in Km²	%
AGRL	Agriculture land	442.6	22.4	199.2	10.1	243.4	12.3
BL	Barren land	613.3	31.0	85.6	4.3	527.7	26.7
BU	Built-up	222.0	11.2	980.5	49.6	-758.5	-38.4
FL	Forest land	94.7	4.8	31.1	1.6	63.6	3.2
GL	Grass land	97.9	5.0	18.6	0.9	79.3	4.1
SL	Shrub land	480.8	24.3	510.9	25.9	-30.1	-1.6
WB	Water body	24.0	1.2	149.3	7.6	-125.3	-6.4
	TOTAL	**1976**	**100**	**1976**	**100**	-	-

3.2.2 Model stream flow response to land use dynamics

The mean annual stream flow response to land use scenarios is summarized in Table 4.19 for the 44 years (1986 LULC-2029 LULC) difference impact of land use dynamics on the stream flow.

Table 4.19: Simulated mean annual stream flow response to land use change.

Time-based Land use	Mean yearly stream flow (m3/s)
Scenario I	136.74
Scenario II	128.20
Scenario III	126.67
Change (I-II) (%)	8.20%
Change (I-III) (%)	10.31%

The results indicated that mean annual stream flow for scenario I (2029 LULC and climate of 2001s) increased by 8.20% than scenario II (1986 LULC and climate of 2002s). This means that the mean annual stream flow of Dabus watershed increased by 10.31% due to land use land cover change only. The main contributing factors for this change were the expansion of the intensive Built-up area and expansion of bare land as compared to 1986 land use land cover.

The combined effect of land use change, climate variability and other factors made the average annual stream flow to increase by 19.3%. Accordingly, the details of the simulated monthly stream flow were compared graphically for the period of (1996-2009) for scenario I (climate of 2000s & 2029 LULC) and scenario II (climate of 2000s & 1986 LULC) as shown in Fig. 4.15.

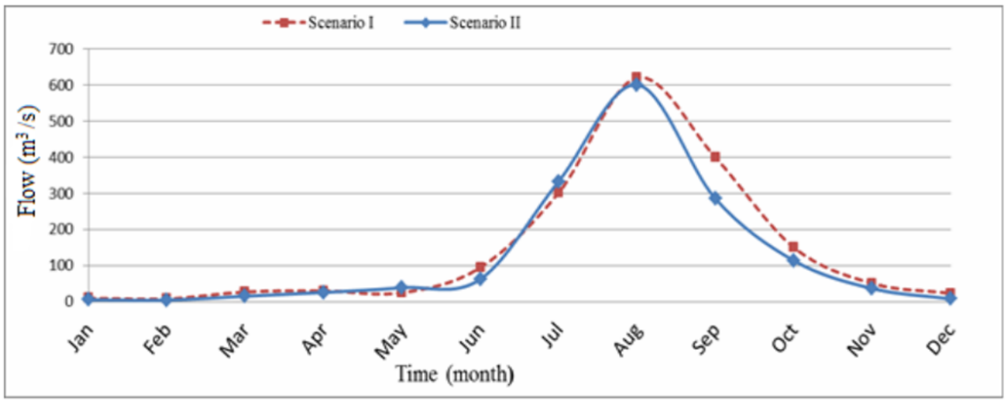

Fig. 4.15: Monthly simulated stream flow variation under LULC for the period of (1996– 2002) for 1986(scenario II) and 2029(scenario I) LULC.

The simulated stream flow hydrograph shown in the Figure 4.15 indicates that the land use dynamics have a higher effect during the peak stream flow season (August) and the medium flow months (September – November). This in turn shows that the surface runoff response to rainfall mainly depends on the characteristics of the watershed. The land use dynamics creates a lower effect on stream flow during the dry season (which is mainly the base flow), as compared to the stream flow during the rainy season. A wide range of changes in stream flow will be experienced between August and October of 2029 LULC compared to the August and October of 1986 LUL. The increase in monthly stream flow is likely to reach up to 25.67 % in September under the same climatic conditions. This is attributed to the expected increase in the area under built up and bare land in 2029 leading to increased runoff.

These findings are in agreement with the results obtained by Alansi (2009), who established that cumulative annual runoff had increased slightly from 1990-1998 compared to 1980-1989, and there was increased runoff during 1990's compared to 1980's at similar rainfall amount. The author related the increase in runoff to the reduction of forest cover during 1990's in Bernam Watershed, Malaysia. In addition, Restrepo and Syvitski (2006) found that most of the tributaries in the upper Magdalena basin experienced momentous rise in sediment load between 1991 and 2001. This was attributed to the severe declining of forest cover compounded with increment of agricultural land cover under the study period. Similarly, Memarian et al. (2012) reported that Surface runoff was increased by 34.6m^3/s as a result of the expansion of built-up area during the study period (1986 – 2011).

3.2.3 Model Sediment yield response to land use dynamics

Like stream flow analysis under land use dynamics discussed above, the impact of land use land cover dynamics in annual sediment yield response of Dabus watershed was evaluated based on the aforementioned three scenarios. The SWAT model simulation results of Dabus watershed indicate that land use change impact on the sediment yield is greater than its effect on the stream flow in the watershed. Sediment yield is expected to increase by 10.39% in 2029 as compared to the sediment yield of 1986 as shown in Table 4.20. This increment may be due to the expansion of intensive built-up area practice in the watershed and existing of large area of bare land within the study area.

Table 4.20: Simulated annual sediment yield response to land use change.

Time-based Land use	Yearly sediment yield (ton/ha)
Scenario I	16.18
Scenario II	13.54
Scenario III	12.87
Change (I-II) (%)	17.39
Change (I-III) (%)	24.80

3.2.4 Seasonal inconsistency of Dabus watershed in sediment yield

The variability of sediment yield on a monthly time scale for the period (1986-20010) for scenario I (weather of 2001s & 2029 LULC) and scenario II (weather of 2002s & 1986 LULC) is presented in Fig 4.16. The results were significant for analyzing the seasonal inconsistency impact of land use land cover dynamics on sediment yield in the study area.

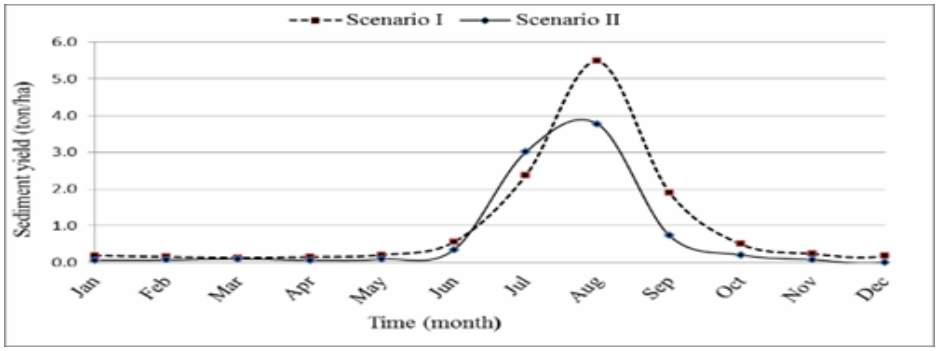

Fig. 4.16: Monthly simulated sediment yield variation under LULC for the period of (1996–2006) for 1986 (scenario I) and 2029 (scenario II) LULC.

The simulated temporal pattern of the sediment outflow from the entire basin of the study area indicates a seasonal variability of the sediment outflow for both land use land cover reference years (1986 LULC and 2029 LULC) using 2001s climatic data. The simulated monthly sediment yield hydrograph shown in the Figure 4.16 indicates that land use dynamics has a higher effect on the peak sediment yield season (August to September), at the season when stream flow is also maximum. The maximum monthly sediment difference between 1986 and 2029 LULC (impact land use dynamics on monthly sediment yield) occurs during September and August at 1.89 and 2.17 ton/ha respectively. These findings are in agreement with the results obtained by Singh1 et al. (2018), who established that cumulative annual sediment outflow had increased slightly from 1997-2000 compared to 1980-1989, and there was increased sediment load during 1997's compared to 1980's at similar rainfall amount. The author related the increase in runoff to the reduction of forest cover during 1997's in Bernam Watershed, Malaysia. In addition, Akyürek et al. (2018) found that most of the tributaries in the upper Magdalena basin experienced momentous rise in sediment load between 1991 and 2001. This was attributed to the severe declining of forest cover compounded with increment of agricultural land cover under the study period. Similarly, Memarian et al. (2013) reported that Surface runoff was increased by 34.t/ha as a result of the expansion of built-up area during the study period (1986 – 2014).

4. Conclusion

Sediment yield season (August to September) at the season when stream is additionally boosted. The most extreme month to month silt yield contrast somewhere in the range of 1986 and 2029 LULC happens at long stretches of September and august as 1.18 and 1.17 t/ha separately. Dabus sub-catchment had encountered noteworthy changes in the land use land spread over the multiyear interim. Among the various sorts of land use, which demonstrate a huge change are developed land and uncovered land (expanded by 8.51% and 0.9%) separately. The primary driver of this huge change was because of development of concentrated agrarian practice in the zone which later causes a fast decrease of bush land and field by 5.62% and 3.33% separately. Woods, water body and manor were likewise demonstrated a huge element during the examination of the multiple times reference land employments. For both reference land utilizes (1986 LULC and 2029 LULC), delicate parameters of stream and residue yield were the equivalent despite the fact that equivalent parameters affectability rank fluctuates. Subsequently, these aligned parameters can be utilized for further future hydrological and natural investigations in the Dabus bowl without expecting to do affectability examination. All the more ever, the appropriateness of the SWAT model in recreating silt release and stream elements of Dabus sub-catchment has approved dependent on the palatable estimations of the factual proportions of the model proficiency. Thus, the model recreation results give certainty to the further utilization of the model to evaluate the hydrologic reaction examination because of spatial and worldly changeability of the catchment attributes will have negligible inclination inside Dabus sub-catchment. The mean yearly stream and yearly silt yield of the watershed demonstrates an expansion in normal yearly stream from 129.20 m3/s to 137.74 m3/s (6.20% augmentation). Also, Sediment yield change demonstrates an augmentation of 17.39% (from 12.54 to 15.17 t/ha). These augmentations of stream and residue yield were exceptionally seen during August to October (substantial precipitation seasons). This is the immediate relationship of silt yield and overflow. For example, residue yield is a capacity spillover and different procedure occurring in the catchment. Nearly the land use elements highly affect dregs yield than stream. Subsequently watershed conditions ought to be ceaselessly evaluated for better administration of the particular watershed.

Acknowledgments

The Authors express their genuine gratitude to the Assosa University for general help to accomplish this logical research.

Author Contributions

Fikereselise Akalu assumed a significant job in the origination of the examination, information assembling and investigations, drafting, translating the outcomes and modifying the composition. Raude, J. M., Eskinder Gidey and Kiptala.J added to supervision and survey this paper. All writers read and endorsed the last original copy.

Conflicts of Interest

The authors declare no conflict of interest.

Reference

1. Agoyi, E. E., Assogbadjo, A. E., Gouwakinnou, G., Okou, F. A. Y., & Sinsin, B. (2014). Ethnobotanical assessment of Moringa oleifera Lam. In Southern Benin (West Africa). Ethnobotany Research and Applications, 12(November), 551–560. https://doi.org/10.17348/era.12.0.551-560
2. Besalatpour, A., Hajabbasi, M. A., Ayoubi, S., & Jalalian, A. (2012). Identification and prioritization of critical sub-basins in a highly mountainous watershed using SWAT model, 1, 58–63.
3. Chhabra, A., Centre, S. A., Houghton, R. A., Hole, W., Braimoh, A. K., Bank, W., & Vlek, P. L. G. (2006). Land-Use and Land-Cover Change. https://doi.org/10.1007/3-540-32202-7
4. Chiwa, R. (2012). Effects of Land Use and Land Cover changes on the hydrology of WeruWeru-Kiladeda sub-catchment in Pangani River Basin, Tanzania. MSc Thesis, Kenyatta University, Kenya, 111pp.
5. FAO. (2011). Strengthening Capacity for Climate Change Adaptation in the Agriculture Sector in Ethiopia. Proceedings from National Workshop Held in Nazreth Ethiopia 5-6 July 2010. https://doi.org/doi.org/10.2499/CAPRiWP83.
6. Joseck Joab, M., Khaemba, A., Mburu, N., & Ngaywa Moses, A. (2016). Effects of increased land use changes on runoff and sediment yield in the Upper River Nzoia Catchment. International Journal of Civil Engineering and Technology (IJCIET), 7(2), 76–94. Retrieved from http://www.iaeme.com/IJCIET/index.asp%0Ahttp://www.iaeme.com/IJCIET/issues.asp%0Awww.jifactor.com%0Ahttp://www.iaeme.com/IJCIET/issues.asp?JType=IJCIET&VType=7&IType=2%0Ahttp://www.iaeme.com/IJCIET/index.asp%5Cnhttp://www.iaeme.com/IJCIET/issues.asp%5Cnww

7. KNMI. (2000). Handbook for the Meteorological Observation. Handbook for the Meteorological Observation, (September), 91–110. Retrieved from http://www.knmi.nl/samenw/hawa/pdf/Handbook_H01_H06.pdf
8. Lenhart, T., Eckhardt, K., Fohrer, N., & Frede, H. (2002). Comparison of two different approaches of sensitivity analysis, 27, 645–654.
9. Li, Z., Liu, W., Zhang, X., & Zheng, F. (2009). Impacts of land use change and climate variability on hydrology in an agricultural catchment on the Loess Plateau of China. Journal of Hydrology, 377(1–2), 35–42. https://doi.org/10.1016/j.jhydrol.2009.08.007
10. Lippmann, R., Haines, J. W., Fried, D. J., Korba, J., & Das, K. (2000). The 1999 {DARPA} off-line intrusion detection evaluation. Comput. Networks, 34(4), 579–595.
11. Mengistu, D. T., & Sorteberg, A. (2012). Sensitivity of SWAT simulated streamflow to climatic changes within the Eastern Nile River basin, 391–407. https://doi.org/10.5194/hess-16-391-2012
12. Moriasi, D. N., Arnold, J. G., Liew, M. W. Van, Bingner, R. L., Harmel, R. D., & Veith, T. L. (2007). M e g s q a w s, 50(3), 885–900.
13. Rao, G. V. R. S. (2015). HYDROLOGICAL IMPACTS DUE TO LAND-USE AND LAND-COVER CHANGES OF KETAR WATERSHED, LAKE ZIWAY CATCHMENT, ETHIOPIA, 6(10), 36–45.
14. Sayemuzzaman, M., & Jha, M. K. (2014). Modeling of Future Land Cover Land Use Change in North Carolina Using Markov Chain and Cellular Automata Model. American Journal of Engineering and Applied Sciences, 7(3), 295–306. https://doi.org/10.3844/ajeassp.2014.295.306
15. Sewnet, A. (2015). c. Journal of Landscape Ecology (Czech Republic), 8(1), 69–83. https://doi.org/10.1515/jlecol-2015-0005
16. Sewnet, A. (2016). Land use/cover change at Infraz watershed by using GIS and remote sensing techniques, northwestern Ethiopia. International Journal of River Basin Management, 14(2), 133–142. https://doi.org/10.1080/15715124.2015.1095199
17. Shen, Z. Y., Gong, Y. W., Li, Y. H., Hong, Q., Xu, L., & Liu, R. M. (2009). A comparison of WEPP and SWAT for modeling soil erosion of the Zhangjiachong Watershed in the Three Gorges Reservoir Area. Agricultural Water Management, 96(10), 1435–1442. https://doi.org/10.1016/j.agwat.2009.04.017
18. Singh, A., Imtiyaz, M., Isaac, R. K., Denis, D. M., Singh, A., Imtiyaz, M., … Assessing, D. M. D. (2014). Assessing the performance and uncertainty analysis of the SWAT and RBNN models for simulation of sediment yield in the Nagwa watershed, India Assessing the performance and uncertainty analysis of the SWAT and. Hydrological Sciences Journal, 59(2), 351–364. https://doi.org/10.1080/02626667.2013.872787
19. Srinivasan, R., Santhi, C., Harmel, R. D., & Griensven, A. Van. (2012). Swat: Model Use, Calibration, And Validation. American Society of Agricultural and Biological Engineers, 55(4), 1491–1508. https://doi.org/ISSN 2151-0032
20. Tuppad, P., Kannan, N., Srinivasan, R., Rossi, C. G., & Arnold, J. G. (2010). Simulation of Agricultural Management Alternatives for Watershed Protection, 3115–3144. https://doi.org/10.1007/s11269-010-9598-8
21. Welde, K., & Gebremariam, B. (2017). Effect of land use land cover dynamics on hydrological response of watershed: Case study of Tekeze Dam watershed, northern Ethiopia. International Soil and Water Conservation Research, 5(1), 1–16. https://doi.org/10.1016/j.iswcr.2017.03.002
22. Wilson, C. O., & Weng, Q. (2011). Simulating the impacts of future land use and climate changes on surface water quality in the Des Plaines River watershed, Chicago Metropolitan Statistical Area, Illinois. Science of the Total Environment, 409(20), 4387–4405. https://doi.org/10.1016/j.scitotenv.2011.07.001